

Research Article

# Effect of Core Size Distribution of Immobilized Magnetic Nanoparticles on Harmonic Magnetization

Takashi Yoshida\* · Teruyoshi Sasayama · Keiji Enpuku

Department of Electrical Engineering, Kyushu University, Japan

\*Corresponding author, email: t\_yoshi@ees.kyushu-u.ac.jp

Received 25 November 2016; Accepted 17 January 2017; Published online 23 March 2017

© 2017 Yoshida; licensee Infinite Science Publishing GmbH

This is an Open Access article distributed under the terms of the Creative Commons Attribution License (<http://creativecommons.org/licenses/by/4.0>), which permits unrestricted use, distribution, and reproduction in any medium, provided the original work is properly cited.

## Abstract

In magnetic particle imaging (MPI), harmonic magnetization signals detected from magnetic nanoparticles (MNPs) are used to image the spatial distribution of the MNPs. The strength of the harmonic signals is directly related to the sensitivity of the MPI system. In this study, we used numerical simulations based on the Fokker-Planck equation to explore the effect of the core size distribution of an immobilized MNP sample on the harmonic signals. We assumed an anisotropy value of  $5 \text{ kJ/m}^3$  and a uniform volume-weighted core size distribution of MNPs ranging from 17.4 to 37.6 nm to simulate a typical MNPs sample. First, we show that the strength of the harmonic signals of the MNP sample were much lower than calculated from the scalar summation of the harmonic signals generated from each MNP in the sample. For example, the strength of the 9th harmonic signal decreased to one-third. This indicates that about 67% of the 9th harmonic signals generated from each MNP are mutually cancelled. We then show that the phase lag of the magnetization due to a finite Néel relaxation time caused lower harmonic magnetization signals of the MNP sample when the core size was distributed. These results indicate that an MNP sample with a narrow size distribution and small anisotropy energy would effectively improve the sensitivity of the MPI system.

## 1. Introduction

Magnetic particle imaging (MPI) is a new modality for imaging the spatial distribution of magnetic nanoparticles (MNPs), and can be used for in-vivo diagnostic applications [1]. In MPI, nonlinear magnetization signals from MNPs under an alternating current (AC) excitation field are detected. Therefore, the performance of MPI strongly depends on the properties of the AC magnetization of the MNPs [2, 3].

The strength of the harmonic signals caused by the nonlinearity of the magnetization is strongly dependent on the core size of the MNP. Therefore, a study is necessary to quantify the dependence of the AC magnetiza-

tion on the core size of the MNP in order to improve the performance of MPI. Ferguson et al. studied the optimal core size of magnetite MNPs for MPI [4]. They modeled the AC magnetization of MNPs using a modified Langevin function that included the effect of the relaxation time. Ludwig et al. evaluated the MPI tracer's core size, hydrodynamic size, and magnetic anisotropy, which are important physical parameters to determine the AC magnetization of MNPs, using AC susceptometry (ACS), magnetorelaxometry (MRX), and magnetic particle spectroscopy (MPS) [5]. Eberbeck et al. introduced a bimodal lognormal distribution of effective core size for Resovist MNPs and showed that the harmonic magnetization spectrum was generated from the larger fraction,

which consisted of the agglomerate of elementary particles [6]. Based on the findings in [6], a magnetically fractionated Ferucarbotran NMP sample was characterized for MPI [7]. The sample included a large portion of particles that are responsible for the harmonic spectrum. As a result, its harmonic spectrum increased by a factor of 2.5 compared with the original sample, indicating that the harmonic spectrum is significantly affected by the distribution of core sizes in a practical MNP sample.

In this study, we use numerical simulations based on the Fokker-Planck equation to study the effect of the core size distribution of an immobilized MNP sample on the harmonic signals. We first present numerical simulation results for an MNP sample with a relatively large core size distribution. We quantify how the core size distribution of the MNP sample affects the harmonic magnetization. It is shown that the phase lag of the magnetization is different for each MNP in the sample because of the core size dependence of the Néel relaxation time. The distribution of the phase lag between the MNPs causes the low harmonic magnetization signals of the MNP sample. Next, we perform a numerical simulation for an MNP sample with a narrow core size distribution. Comparing the results obtained for the two cases, we quantify the effect of the core size distribution on the harmonic magnetization.

## II. Material and Methods

### II.1. Numerical Simulations

Micro-magnetic simulations are usually used to study the dynamic behavior of MNPs [8, 9]. The behavior of MNPs obeying the Néel mechanism can be described by the Fokker-Planck equation [10]:

$$2\tau_{N0}\sigma\frac{\partial W}{\partial t} = \frac{1}{\sin\theta}\frac{\partial}{\partial\theta}\left\{\sin\theta\left[\frac{1}{k_B T}\left(\frac{\partial E}{\partial\theta} - \frac{1}{\sin\theta}\frac{1}{\alpha}\dots\right.\right.\right. \\ \left.\left.\left.\dots\frac{\partial E}{\partial\phi}\right)W + \frac{\partial W}{\partial\theta}\right]\right\} + \frac{1}{\sin\theta}\frac{\partial}{\partial\phi}\left\{\frac{1}{k_B T}\left(\frac{1}{\alpha}\frac{\partial E}{\partial\theta}\dots\right.\right. \\ \left.\left.\dots + \frac{1}{\sin\theta}\frac{\partial E}{\partial\phi}\right)W + \frac{1}{\sin\theta}\frac{\partial W}{\partial\phi}\right\}. \quad (1)$$

Here,  $\tau_{N0}$  is the characteristic Néel relaxation time,  $\sigma = KV_c/k_B T$  is the anisotropy energy barrier normalized by the thermal energy  $k_B T$ ,  $K$  is the anisotropy constant,  $V_c$  is the core volume of the MNP,  $\theta$  and  $\phi$  are polar and azimuthal angles, respectively,  $W(\theta, \phi, t)$  is the distribution function of magnetic moment  $m$ , and  $\alpha$  is a dimensionless damping factor. In the numerical simulation,  $\tau_{N0} = 10^{-9}$  and  $\alpha$  was assumed to be sufficiently large to neglect the contribution from the precession term in Eq. (1), i.e., numerical calculations were performed for the high damping limit [11].

When the easy axis of the MNP is defined to be the  $z$ -direction and an AC excitation field  $H(t) = H_{ac} \cos 2\pi f t$  is applied in the  $xz$ -plane with an angle  $\beta$  relative to the  $z$ -axis, the potential energy of the MNP is given by

$$E = -\mu_0 M_s V_c H (\sin\beta \sin\theta \cos\phi + \cos\beta \cos\theta) \dots \\ \dots + KV_c \sin^2\theta. \quad (2)$$

Here,  $M_s = m/V_c$  is the saturation magnetization. In the numerical simulation, we set  $M_s = 360$  kA/m,  $K = 5$  kJ/m<sup>3</sup>, and  $T = 300$  K.

By using the matrix continued fraction technique [12], we can calculate the  $k$ -th harmonic of the complex magnetization in the direction of the AC excitation field,  $M_{k\beta}$ . Details of the simulation procedure were published elsewhere [13]. For the case when the easy axes of the MNPs are randomly oriented, the  $k$ -th harmonic of the complex magnetization of MNPs with core size  $d_c$ , designated by  $M_k(d_c)$ , was calculated as follows:

$$M_k(d_c) = \sum_{j=1}^M \sum_{i=1}^N M_{k\beta}(\beta_i) \sin\beta_i \Delta\beta, \quad (3)$$

where  $\beta_i = \pi(i - 0.5)/2N$ . In the numerical simulation, we set  $N = 90$  and  $\Delta\beta = \pi/180$ .

### II.2. Core Size Distribution

When a core size distribution exists in the MNP sample, the total  $k$ -th harmonic of the complex magnetization,  $\langle M_k \rangle$ , is given by the following equation

$$\langle M_k \rangle = \frac{\sum_i f(d_{ci}) V_{ci} M_k(d_{ci}) \Delta d_{ci}}{\sum_i f(d_{ci}) V_{ci} \Delta d_{ci}}. \quad (4)$$

Here,  $V_{ci}$  is the core volume of the MNP,  $f(d_{ci})$  is the number of MNPs within distance  $\Delta d_{ci}$  around  $d_{ci}$ . In the simulation, for simplicity, we assumed a uniform volume-weighted core size distribution. Namely, we assume the value of  $f(d_{ci}) V_{ci}$  to be constant, ranging from  $d_{c\min}$  to  $d_{c\max}$ . Here,  $d_{c\min}$  and  $d_{c\max}$  are the minimum and maximum values of the core size, respectively.

We obtain the real  $\langle M_k \rangle'$  and imaginary  $\langle M_k \rangle''$  parts and the phase lag  $\phi_k$  of the  $k$ -th harmonic magnetization as follows:

$$\langle M_k \rangle = \langle M_k \rangle' - j \langle M_k \rangle'', \quad (5)$$

$$\phi_k = \tan^{-1}(\langle M_k \rangle'' / \langle M_k \rangle') + n\pi, \quad (6)$$

where the first term of Eq. (6) is defined in the region  $[-\pi/2, \pi/2]$ , and  $n$  is integer: the value of  $n = 0$  is usually selected.

## III. Results and Discussion

We first performed a numerical simulation for a case of  $d_{c\min} = 17.4$  nm and  $d_{c\max} = 37.6$  nm. These values

were chosen based on the core size distribution of a practical MNP sample (Resovist, FUJIFILM Pharma). Using a relationship of  $m = M_s \frac{\pi}{6} d_c^3$ , the minimum and maximum values of magnetic moment are calculated as  $m_{\min} = 10^{-18} \text{ Am}^2$  and  $m_{\max} = 10^{-17} \text{ Am}^2$ , respectively.

The filled circles in Fig. 1 represent the amplitude of the harmonic signals of the MNP sample when an AC excitation field with amplitude  $\mu_0 H_{ac} = 20 \text{ mT}$  and frequency  $f = 20 \text{ kHz}$  is applied. As can be seen, the amplitude of the harmonic magnetization decreases monotonically with increasing harmonics number  $k$ . For comparison, we calculated the scalar summation of the amplitude of the harmonic magnetization signal generated from each MNP,  $\langle M_k \rangle_{ss}$ . We note that  $M_k(d_{ci})$  in Eq. (4) is a complex value. The scalar summation is given by:

$$\langle M_k \rangle_{ss} = \frac{\sum_i f(d_{ci}) V_{ci} |M_k(d_{ci})| \Delta d_{ci}}{\sum_i f(d_{ci}) V_{ci} \Delta d_{ci}}, \quad (7)$$

where  $|M_k(d_{ci})|$  is the amplitude of the  $k$ -th harmonic magnetization of the MNP with core size  $d_{ci}$ .

As shown in Fig. 1, the amplitude of the harmonic signal of the MNP sample (filled circles) is much lower than that calculated from the scalar summation of the amplitude of the harmonic signals generated from each MNP (open circles). For example, the strength of the 9th harmonic signal decreases to one-third. This indicates that about 67% of the 9th harmonic magnetization signals from each MNP are mutually cancelled.

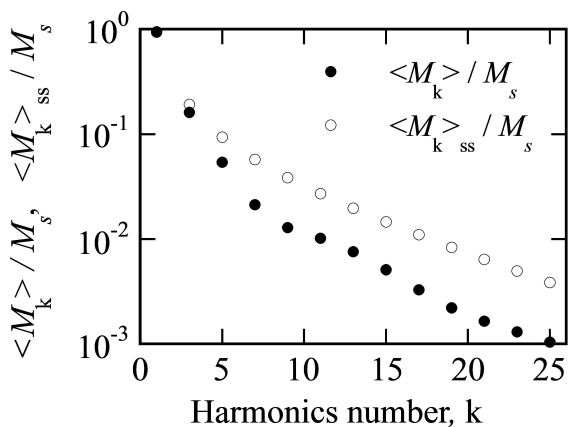


**Figure 1:** Amplitude of the harmonic magnetization spectrum when an AC excitation field with amplitude  $\mu_0 H_{ac} = 20 \text{ mT}$  and frequency  $f = 20 \text{ kHz}$  was applied. A uniform volume-weighted core size distribution ranging from 17.4 nm to 37.6 nm was assumed. Filled circles represent the harmonic spectrum calculated using Eq. (4). Open circles represent the scalar summation of the amplitude of harmonic signals generated from each MNP calculated using Eq. (7).

In order to determine the origin of the decrease in the strength of the harmonic magnetization, we show the AC magnetization curves for  $d_c = 20 \text{ nm}$  and  $d_c = 35 \text{ nm}$

in Fig. 2. As can be seen, the AC magnetization for  $d_c = 20 \text{ nm}$  occurs without a phase lag, while that for  $d_c = 35 \text{ nm}$  occurs with a large phase lag. This difference can be explained by the Néel relaxation time. Using an analytical expression, Brown's field-dependent Néel relaxation time is given by [10]

$$\tau_N(\xi, \sigma) = \frac{\sqrt{\pi}}{2\sqrt{\sigma}} \tau_{N0} \frac{e^{\sigma(1+h^2)}}{(1-h^2)(\cosh \xi - h \sinh \xi)} \quad (8)$$

with  $h = \xi/2\sigma$  and  $\xi = \mu_0 H_{ac} m / \sqrt{2} k_B T$ , the Néel relaxation time for  $d_c = 20 \text{ nm}$  is calculated as  $7.3 \cdot 10^{-9} \text{ s}$ . Since this value is much shorter than the change of the AC excitation field of  $\frac{1}{2\pi f} = 8 \cdot 10^{-6} \text{ s}$ , the phase lag is negligible in this case. On the other hand, the Néel relaxation time for  $d_c = 35 \text{ nm}$  is calculated as  $6.5 \cdot 10^{-7} \text{ s}$ . In this case, the relaxation time cannot be neglected, and as a result, the AC magnetization for  $d_c = 35 \text{ nm}$  occurs with a large hysteresis area and a phase lag.

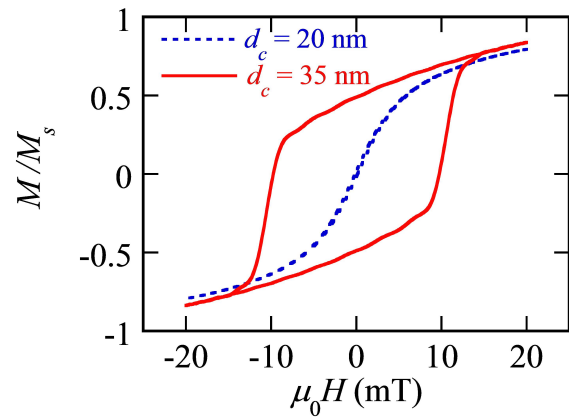


**Figure 2:** AC magnetizations of MNPs with  $d_c = 20 \text{ nm}$  and  $d_c = 35 \text{ nm}$ , when an AC excitation field with amplitude  $\mu_0 H_{ac} = 20 \text{ mT}$  and frequency  $f = 20 \text{ kHz}$  was applied.

Figure 3 shows the dependence of the phase lag of the harmonic magnetization,  $\phi_k$ , on the core size  $d_c$ . As shown,  $\phi_k$  increases with increasing  $d_c$ , and its dependence becomes stronger for higher harmonics number  $k$ . We note that the value of  $n$  in Eq. (6) was chosen so as to obtain a smooth  $d_c$  vs.  $\phi_k$  curve. For example, we first selected  $n = 0$  for small  $d_c$  values. The value of  $\phi_k$  increased with increasing  $d_c$ , and reached to  $\pi/2$ . Then, we selected  $n = 1$  for the following  $d_c$  values. If we keep  $n = 0$  for all values,  $d_c$  vs.  $\phi_k$  curve becomes a saw-tooth like curve.

We note that  $M_k(d_{ci})$  in Eq. (4) is a complex value. When a phase lag exists, the real and imaginary parts of  $M_k(d_{ci})$  become positive or negative depending on the value of  $\phi_k$ . Since the value of  $\phi_k$  changes with the core size as shown in Fig. 3, the real and imaginary parts of  $M_k(d_{ci})$  depend on the core size. In Fig. 4, the dependence of the real  $M'_k$  and imaginary  $M''_k$  parts of the 9th

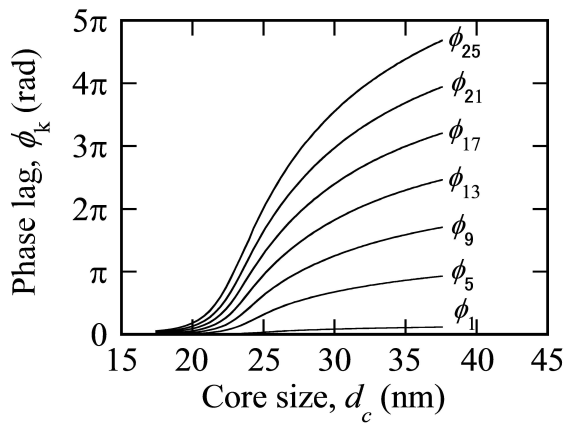


**Figure 3:** Dependence of the phase lag of the harmonic magnetization on the core size.

harmonic magnetization on the core size are shown. As expected from the  $d_c$  vs.  $\phi_k$  curve shown in Fig. 3, both  $M_9'$  and  $M_9''$  become positive or negative depending on the core size. This means that the harmonic magnetization signals from each MNP are mutually cancelled when the core size is distributed in the MNP sample. This is the reason for the degradation of the harmonic spectra of the MNP sample when the core size is distributed.

We note that experimental results of harmonic spectra of Resovist sample agreed well with the numerical simulation when the actual distribution of core size was taken into account [13].

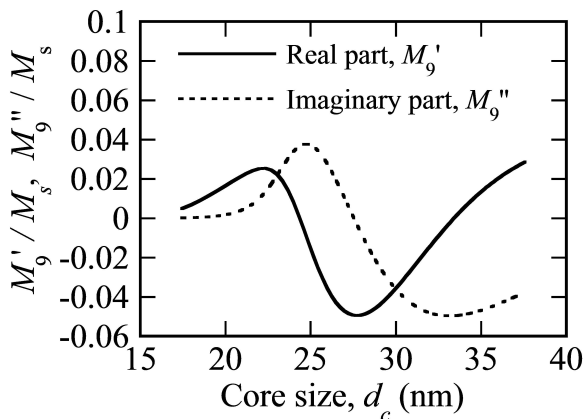


**Figure 4:** Dependence of the real  $M_9'$  and imaginary  $M_9''$  parts of the 9th harmonic magnetization on the core size.

We also note that the  $d_c$  vs.  $\phi_k$  curve shown in Fig. 3 depends on the value of the anisotropy energy constant  $K$ ; the value of  $\phi_k$  decreases with decreasing  $K$ . Therefore, an MNP with a small value of  $K$  can be used to prevent the degradation of the harmonic spectra due to core size distribution.

Finally, we performed a numerical simulation for a case with  $d_{c\min} = 25$  nm and  $d_{c\max} = 30$  nm. In this case, the range of the core size distribution was one-quarter the previous case, while the mean core size remained the same. In Fig. 5, comparison of the amplitude of the harmonic signals between the two cases is shown. The open squares in Fig. 5 represent an MNP sample with  $d_{c\min} = 25$  nm and  $d_{c\max} = 30$  nm, while the filled circles represent an MNP sample with  $d_{c\min} = 17.4$  nm and  $d_{c\max} = 37.6$  nm. As shown, the strength of the harmonic magnetization is larger for the MNP sample with a narrow size distribution. This is because the phase lag  $\phi_k$  remains in a narrow range, as can be seen in Fig. 3. For example, a 3.2-fold increase was observed in the 9th harmonic magnetization from the MNP sample with a narrow core size distribution compared with the MNP sample with a wider core size distribution. This result indicates that an MNP sample with a narrow size distribution improves the sensitivity of the MPI system.

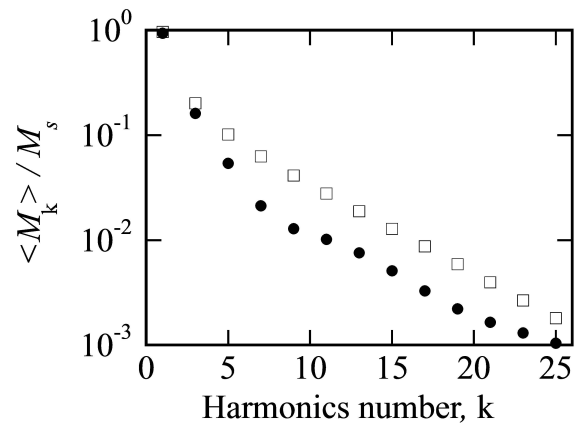


**Figure 5:** Amplitude of the harmonic magnetization spectrum when an AC excitation field with amplitude  $\mu_0 H_{ac} = 20$  mT and frequency  $f = 20$  kHz was applied. Open squares and filled circles are for MNP samples with a uniform volume-weighted core size distribution ranging from 25 to 30 nm, and from 17.4 nm to 37.6 nm, respectively.

## IV. Conclusion

We used numerical simulations based on the Fokker-Planck equation to explore the effect of the core size distribution of an immobilized MNP sample on the harmonic magnetization signals. First, we showed that the strength of the harmonic signals of the MNP sample were much lower than calculated from the scalar summation of the harmonic signals generated from each MNP in the sample. This degradation indicated that the harmonic signals from each MNP were mutually cancelled, and was caused by the difference in the phase lag between each

MNP. It was also shown that the amplitude of the harmonic signals increased when the core size distribution was narrow. These results indicate that an MNP sample with a narrow size distribution and small anisotropy energy would effectively improve the sensitivity of the MPI system.

## Acknowledgment

This work was supported by the JSPS KAKENHI (15H05764 and 16K14277).

## References

- [1] B. Gleich and J. Weizenecker. Tomographic imaging using the nonlinear response of magnetic particles. *Nature*, 435(7046):1214–1217, 2005. doi:[10.1038/nature03808](https://doi.org/10.1038/nature03808).
- [2] M. Graeser, K. Bente, and T. M. Buzug. Dynamic single-domain particle model for magnetite particles with combined crystalline and shape anisotropy. *J. Phys. D: Appl. Phys.*, 48(27):275001, 2015. doi:[10.1088/0022-3727/48/27/275001](https://doi.org/10.1088/0022-3727/48/27/275001).
- [3] S. A. Shah, D. B. Reeves, R. M. Ferguson, J. B. Weaver, and K. M. Krishnan. Mixed Brownian alignment and Néel rotations in superparamagnetic iron oxide nanoparticle suspensions driven by an ac field. *Phys. Rev. B*, 92(9):094438, 2015. doi:[10.1103/PhysRevB.92.094438](https://doi.org/10.1103/PhysRevB.92.094438).
- [4] R. M. Ferguson, K. R. Minard, and K. M. Krishnan. Optimization of nanoparticle core size for magnetic particle imaging. *J. Magn. Magn. Mater.*, 321(10):1548–1551, 2009. doi:[10.1016/j.jmmm.2009.02.083](https://doi.org/10.1016/j.jmmm.2009.02.083).
- [5] F. Ludwig, H. Remmer, C. Kuhlmann, T. Wawrzik, H. Arami, R. M. Ferguson, and K. M. Krishnan. Self-consistent magnetic properties of magnetite tracers optimized for magnetic particle imaging measured by ac susceptometry, magnetorelaxometry and magnetic particle spectroscopy. *J. Magn. Magn. Mater.*, 360:169–173, 2014. doi:[10.1016/j.jmmm.2014.02.020](https://doi.org/10.1016/j.jmmm.2014.02.020).
- [6] D. Eberbeck, F. Wiekhorst, S. Wagner, and L. Trahms. How the size distribution of magnetic nanoparticles determines their magnetic particle imaging performance. *Appl. Phys. Lett.*, 98(18):182502, 2011. doi:[10.1063/1.3586776](https://doi.org/10.1063/1.3586776).
- [7] T. Yoshida, N. B. Othman, and K. Enpuku. Characterization of magnetically fractionated magnetic nanoparticles for magnetic particle imaging. *J. Appl. Phys.*, 114(17):173908, 2013. doi:[10.1063/1.4829484](https://doi.org/10.1063/1.4829484).
- [8] J. Weizenecker, B. Gleich, J. Rahmer, and J. Borgert. Particle dynamics of mono-domain particles in magnetic particle imaging. In *International Workshop on Magnetic Particle Imaging*, page 6, 2010.
- [9] J. Weizenecker, B. Gleich, J. Rahmer, and J. Borgert. Micro-magnetic simulation study on the magnetic particle imaging performance of anisotropic mono-domain particles. *Phys. Med. Biol.*, 57(22):7317–7327, 2012. doi:[10.1088/0031-9155/57/22/7317](https://doi.org/10.1088/0031-9155/57/22/7317).
- [10] W. T. Coffey, P. J. Clegg, and Y. P. Kalmykov. *Advances in Chemical Physics*, volume 83. Wiley, New York, 1993. doi:[10.1002/SERIES2007](https://doi.org/10.1002/SERIES2007).
- [11] I. S. Poperechny, Y. L. Raikher, and V. I. Stepanov. Dynamic magnetic hysteresis in single-domain particles with uniaxial anisotropy. *Phys. Rev. B*, 82(17):174423, 2010. doi:[10.1103/PhysRevB.82.174423](https://doi.org/10.1103/PhysRevB.82.174423).
- [12] J. L. Dejardin and Y. P. Kalmykov. Nonlinear dielectric relaxation of polar molecules in a strong ac electric field: steady state response. *Phys Rev E Stat Nonlin Soft Matter Phys*, 61(2):1211, 2000. doi:[10.1103/PhysRevE.61.1211](https://doi.org/10.1103/PhysRevE.61.1211).
- [13] T. Yoshida, Y. Matsugi, N. Tsujimura, T. Sasayama, K. Enpuku, T. Viereck, M. Schilling, and F. Ludwig. Effect of alignment of easy axes on dynamic magnetization of immobilized magnetic nanoparticles. *J. Magn. Magn. Mater.*, 427:162–167, 2017. doi:[10.1016/j.jmmm.2016.10.040](https://doi.org/10.1016/j.jmmm.2016.10.040).